Simulation of e-cloud driven instability and its attenuation using a simulated feedback system in the CERN SPS*

J.-L. Vay† and M. A. Furman
Lawrence Berkeley National Laboratory, USA

Electron clouds have been shown to trigger fast growing instabilities on proton beams circulating in the SPS, and a feedback system to control the single-bunch instabilities is under active development. We present the latest improvements to the WARP-POSINST simulation framework and feedback model, and its application to the self-consistent simulations of two consecutive bunches interacting with an electron cloud in the SPS. Simulations using an idealized feedback system exhibit adequate mitigation of the instability providing that the cutoff of the feedback bandwidth is at or above 450 MHz. Artifacts from numerical noise of the injected distribution of electrons in the modeling of portions of bunch trains are discussed, and benchmarking of WARP against POSINST and HEADTAIL are presented.

I. INTRODUCTION

Various methods are being employed to prevent the buildup of electron clouds in particle beam accelerators from reaching critical densities above which they can affect the beam quality, such as surface scrubbing, coating, grooving, etc. [1] However, these methods may be time consuming and expensive, and it is unclear if they can be sufficient for all the configurations that are planned for the near-future. As a complement (or eventually replacement) to the abovementioned techniques for buildup reduction, it has been proposed recently to mitigate the coherent effect of electron clouds on the bunches by using feedback systems [2, 3].

Preliminary simulations of an idealized feedback model for controlling electron cloud driven single bunch instabilities in the SPS [4] have been reported in [5, 6], where the dynamic of a single bunch interacting with a prescribed electron cloud was considered. In this paper, we extend the investigation using computer simulations of electron cloud buildup in the SPS, its effect on two consecutive bunches, and its mitigation using idealized feedback models, considering beams at injection energy of 26 GeV.

The paper is organized as follows: the different modes of operation of the package WARP-POSINST are presented, as well as the latest improvements, in Section II. An idealized feedback system that was implemented in the package is discussed in Section III and is applied to the damping of an ecloud driven instability in Section IV. Section V discusses the influence of numerical noise in the injected distribution of electrons.

* Supported by the US-DOE under Contract DE-AC02-05CH1123, the US-LHC Accelerator Research Program (LARP) and the SciDAC/ComPASS project. Used resources of NERSC and the Lawrencium cluster at LBNL.

† jlvay@lbl.gov

II. THE WARP-POSINST PACKAGE

At PAC05 [7] and PAC07 [8], we presented the package WARP-POSINST for the modeling of the effect of electron clouds on high-energy beams. We present here the latest developments in the package. Three new modes of operations were implemented: 1) a build-up mode where, similarly to POSINST [9–12], ECLOUD (CERN) or Cloudland (SLAC), the build-up of electron clouds driven by a legislated bunch train is modeled in one region of an accelerator; 2) a quasi-static mode [13] where, similarly to HEADTAIL (CERN) [14], QuickPIC (USC/UCLA) [15], PEHTS (KEK) [17] or CMAD (SLAC) [18], the frozen beam approximation is used to split the modeling of the beam and the electrons into two components evolving on their respective time scales; and 3) a "Lorentz boosted mode" where the simulation is performed in a moving frame where the space and time scales related to the beam and electron dynamics fall in the same range. The implementation of mode (1) was primary motivated by the need for benchmarking with other codes, while the implementation of modes (2) and (3) fulfill the drive toward fully self-consistent simulations of e-cloud effects on the beam including the buildup phase. The three modes are described in more details below. Benchmarking of modes (1) and (2) against POSINST and HEADTAIL are given in Appendix.

A. Build-up mode

In the build-up mode, the dynamics of electrons is followed for a thin (2-D) or thick (3-D) slice located at a given location in the lattice, under the influence of a legislated particle beam passing through the slice (Fig. 1). The electrons are described by a collection of macroparticles evolving under the influence of their own space charge, plus the field of an external beam, following the standard Particle-In-Cell (PIC) technique. The electron electric field is obtained in the static approximation from solving the Poisson equation. The field from the external (positively charged) beam is either prescribed analyti-

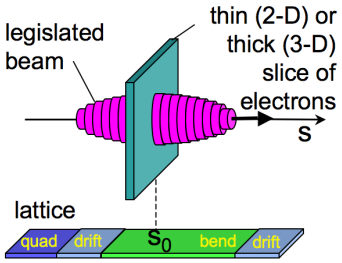

FIG. 1. Sketch of the build-up mode. The dynamics of electrons is followed for a thin (2-D) or thick (3-D) slice located at a given location in the lattice, under the influence of a legislated particle beam passing through the slice.

cally (using the Bassetti-Erskine formula) or given from solving the Poisson equation over a prescribed charge distribution. Benchmarking of the build-up mode against POSINST is given in Appendix A.

B. Quasistatic mode

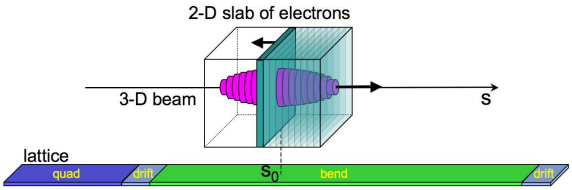

FIG. 2. Sketch of the quasistatic mode. A 2-D slab of electron macroparticles is stepped backward (with small time steps) through the beam field. The 2-D electron fields (solved at each step) are stacked in a 3-D array, that is used to give a kick to the beam. Finally, the beam particles are pushed forward (with larger time steps) to the next station of electrons.

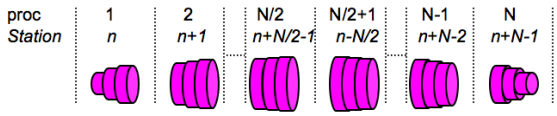

FIG. 3. Sketch of the parallel decomposition for the quasistatic mode. The beam is distributed among n slices, that are uniformly spread among N processors. Using a pipelining algorithm, slices on a given processor are pushed from one station to the next, without waiting for the slices of the previous processors to reach the same station.

In the quasistatic mode, a 2-D slab of electron macroparticles is stepped backward (with small time steps) through the beam field (see Fig. 2). The 2-D electron fields (solved at each step) are stacked in a 3-D array, that is used to give a kick to the beam. Finally, the beam particles are pushed forward (with larger time steps) to the next station of electrons, using either maps or a Leap-Frog pusher. The first implementation was for accelerator lattices treated in the smooth approximation. A more detailed lattice description was implemented later (to be described elsewhere). This mode allows for direct comparison with the quasistatic codes HEADTAIL [14], QuickPIC [15], PEHTS [17] or CMAD [18]. The parallelization is mono-dimensional (along s) using pipelining, similarly to QuickPIC [16]. Assuming that the beam is distributed among n slices of equal thickness along the longitudinal dimension, and that N processors are used for a run, n/N consecutive slices are assigned to each processor, as sketched in Fig. 3. During the first iteration, the electron distribution from the first station in the ring is evolved through the slices of processor N while processors 1 through $N-1$ stay idle. The electron distribution is then passed to processor $N-1$ and evolves through the slices that it contains, while processor N pushes the beam to station 2 and starts evolving the corresponding distribution of electrons. After N steps, all processors are active and the procedure is repeated until the beam slices on processor 1 reach the desired number of turns.

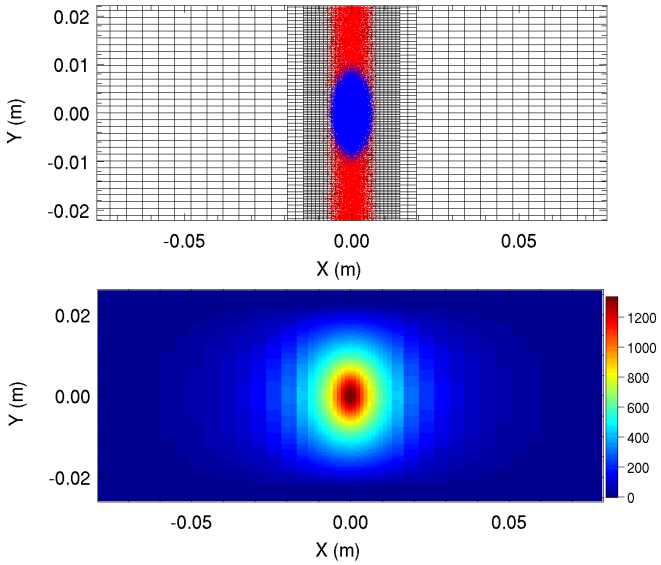

FIG. 4. (top) Snapshot of grid lines (black) using two levels of mesh refinement. The coarse mesh covers the entire SPS pipe cross section, providing adequate boundary conditions for the refined patches covering the area surrounding the electrons (red) and proton beam (blue); (bottom) beam potential in Volts.

Recently, improvements to the quasistatic model have been made toward higher efficiency, enabling self-consistent modeling of multi-bunch effects. Several features that exist in the WARP [19] or POSINST core capability have been made accessible to the WARP-POSINST quasistatic model: mesh refinement, enabling more efficient field solving by concentrating the resolution where it is most needed (See Fig. 4); secondary emission of electrons at the walls; background gas ionization; and the option for using either POSINST or WARP routines for pushing electrons and detecting collisions at the cham-

ber wall. In addition, multi-bunch simulations were enabled with minimal modification of the quasistatic computer code, by taking advantage of MPI groups and communicators features, allowing the diagnostics message-passing routines to handle separate bunches independently. Benchmarking of the quasistatic mode against HEADTAIL on the modeling of single bunch instability is given in Appendix B.

C. Boosted frame approach

It was shown in [20] that it was possible to perform simulations of electron-driven instabilities from first principles (e.g. using standard Particle-In-Cell methods without using the quasistatic approximation), at much reduced computing cost than using "standard" PIC simulations using the laboratory frame as the frame of calculation, by performing the calculation in a suitable Lorentz boosted frame. Numerical developments that were needed have been implemented, including a new particle pusher and field solver, and are described in [21]. Special handling of inputs and outputs between the boosted frame and the laboratory frame are described in [22]. The quasistatic and the boosted frame methods are expected to give similar performances for given resolutions, macroparticles statistics and number of stations per turns, provided that the betatron motion is resolved. This was verified in [21] where two WARP calculations of an electron cloud driven instability showed very good agreement [21] between a full PIC calculation in a boosted frame and a calculation using the quasistatic mode, for similar computational cost. When the betatron motion is not resolved, as has often been the case in past electron cloud driven instability simulations where as little as 1 station per turn has sometimes been used, the quasistatic approach offers no restriction on the choice of number of stations for a given lattice, while the boosted frame approach imposes to adjust either the number of stations or the integer and/or fractional part of the betatron tune. Because of this restriction, coupled to the fact that the quasistatic approach has been used universally by other codes for electron cloud driven instability simulations thus offering more direct benchmarking opportunities, and also because the level of effort alloted for code development did not permit to follow both tracks at the same level, it was chosen to apply only the quasistatic mode for the studies that are reported in this paper. As simulations progress toward higher fidelity by resolving the betatron motion adequately, the boosted frame approach is expected to become a very attractive alternative to the quasistatic approach.

III. FEEDBACK MODEL

The feedback model is a generalization of the model presented in [24], allowing the placement of the feedback kicker at any location in the ring, and the kick to be applied an arbitrary number of turns following the latest measurements. Assuming two measurements of the average transverse displacement y_{i-1} and y_i for a given slice of the bunch at two consecutive turns $i-1$ and i, the predicted average velocity offset of the slice at turn $i+\xi$ (the prediction is made at a different location when ξ is not an integer) is given, using the smooth focusing approximation, by

$$y'_{i+\xi} = \frac{(cc_\xi - ss_\xi)\, y_i - cy_{i-1}}{\beta_y s} \tag{1}$$

where $c = \cos(2\pi Q_y)$, $s = \sin(2\pi Q_y)$, $c_\xi = \cos(2\pi\xi Q_y)$, $s_\xi = \sin(2\pi\xi Q_y)$, and Q_y and β_y are respectively the vertical tune and the beta function. A gain g is assumed and the correction applied at ξ on the bunch slice is given by $\Delta y'_{i+\xi} = -g y'_{i+\xi}$. For $\xi = 0$, the correction is applied at the same location and time of the second measurement and reduces to the formula given in [24]. $\xi = 1$ was used in the calculations presented in this paper, meaning that the correction was applied at the location of the measurements, with one turn delay. A wideband digital filter is optionally used for emulating the finite bandwidth response of a real system.

IV. APPLICATION TO THE STUDY OF E-CLOUD EFFECTS IN THE SPS

TABLE I. Parameters Used for WARP-POSINST Simulations of Ecloud Driven Instability in the SPS

beam energy	E_b	26 GeV
bunch population	N_b	1.1×10^{11}
rms bunch length	σ_z	0.23 m
rms transverse emittance	$\epsilon_{x,y}$	2.8, 2.8 mm.mrad
rms momentum spread	δ_{rms}	2×10^{-3}
bunch spacing	Δ_b	25 ns
beta functions	$\beta_{x,y}$	33.85, 71.87 m
betatron tunes	$Q_{x,y}$	26.13, 26.185
chromaticities	$Q'_{x,y}$	0, 0
Cavity voltage	V	2 MV
momentum compact. factor	α	1.92×10^{-3}
circumference	C	6.911 km
# of bunch slices/bucket	N_{slices}	64
# of stations/turn	N_s	10

The beam-electron-cloud interaction is simulated using the quasistatic model by a succession of N_s discrete interactions around the ring ("ecloud stations") and a smooth approximation for the external focusing from the lattice. The modeling of two consecutive bunches propagating in the SPS at injection was performed using the parameters from Table 1. In order to provide a consistent initial electron distribution, a prior build-up simulation using the code POSINST [25] was performed for a full train of bunches (assuming a secondary electron yield of 1.2 at the walls), and the electron distribution was dumped

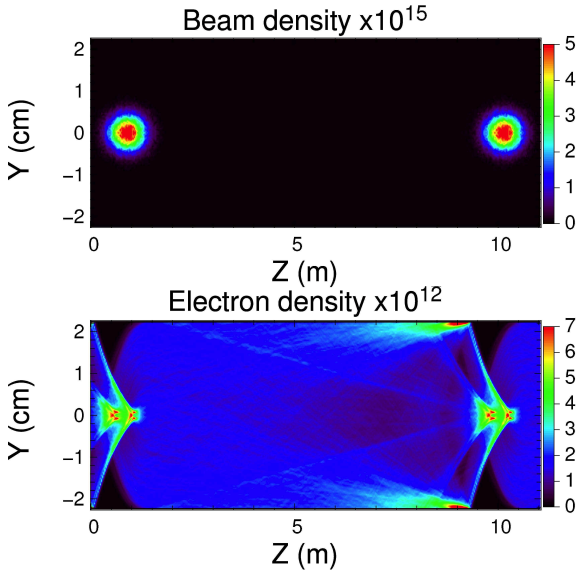

FIG. 5. Number density (in m^{-3}) in the central vertical plane for the bunches (top) and the electrons (bottom). The bunches move from left to right, i.e. bunch 35 is on the right and bunch 36 is on the left.

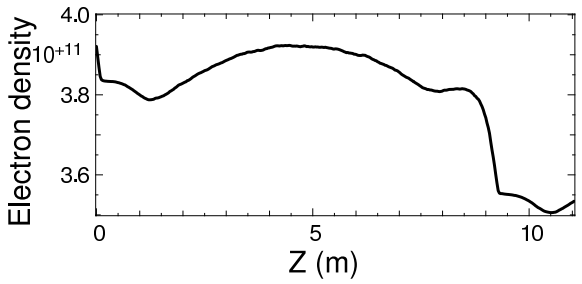

FIG. 6. Number density (in m^{-3}) averaged over the pipe section.

after the passage of bunch 34, chosen so that the electron induced tune shift of the subsequent bunches was commensurate with experimental data [3]. This particle dump was then used to initialize the WARP-POSINST simulation of bunches 35 through 36 (i.e. 6 buckets of 25 ns).

Figure 5 shows a snapshot of the bunches and electron densities in the vertical plane, right after the passage of the bunches through the first station. The electron wake exhibits the focusing of the electrons by the bunches, producing high density spikes which result in jets of electrons impacting the walls and generating secondaries, eventually relaxing to a nearly uniform background. A plot of the electron density averaged over the pipe section is given in Fig. 6, revealing that the average electron density rises by about 8% from bunch 35 to 36.

Simulations were performed with the feedback turned OFF or ON, with gains g=0.1 and g=0.2. The relative vertical emittance growth is shown in Fig. 7 (top) for the two simulated bunches. Both bunches experience a very

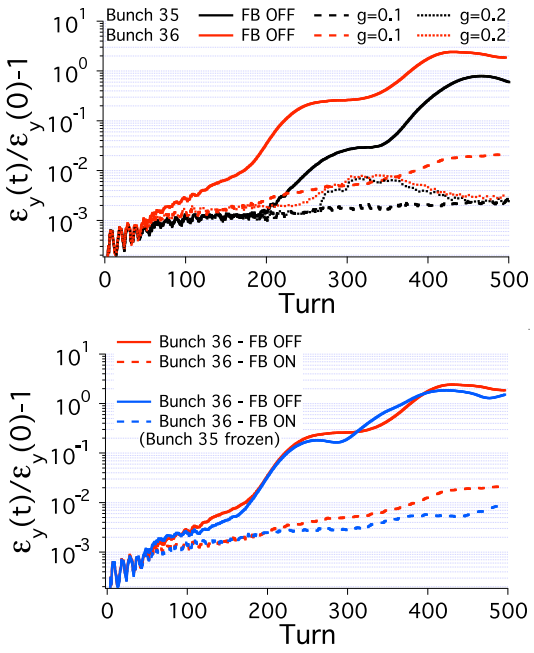

FIG. 7. Relative emittance growth vs turn for: (top) bunches 35 (black) and 36 (red) with feedback OFF (solid) and ON with gain g=0.1 (dash) and g=0.2 (dot); (bottom) bunch 36 with full dynamics for bunch 35 (red) or a non-dynamical ("frozen") bunch 35 (blue) with feedback OFF (solid) and ON (dash) with gain g=0.1.

rapid emittance growth when the feedback is off, which is heavily damped by the simulated feedback. Simulations with the feedback OFF and the feedback ON with g=0.1 were repeated with bunch 35 being frozen. The resulting emittance growth of bunch 36 are contrasted in Fig. 7 (bottom) with the ones obtained previously, showing similar emittance growth, and thus a weak influence of bunch 35 on 36.

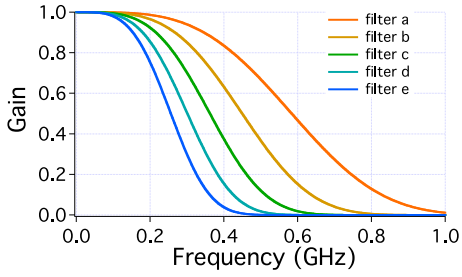

FIG. 8. Frequency response of filters used in simulations with cutoffs (at -3dB) ranging from 250 MHz to 575 MHz.

In the simulations presented so far, the full bandwidth of the measured transverse displacement along the bunch slices was used to predict the feedback correction, without any filtering. However, a real feedback system will have a finite bandwidth. The simulations with the feedback turned ON with g=0.1 were repeated using five fil-

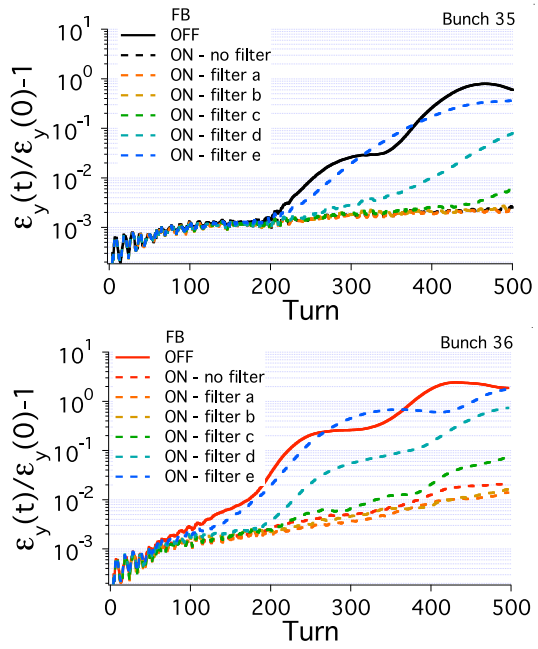

FIG. 9. Relative emittance growth vs turn for bunches 35 (top) and 36 (bottom) with feedback OFF (solid) and ON (dash) with gain g=0.1 and various filters.

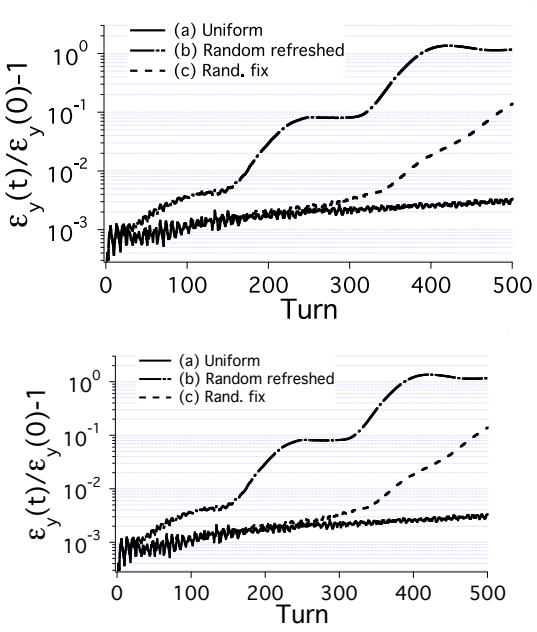

FIG. 10. Relative emittance growth for single bunch simulations with various methods for injecting electrons.

ters with cutoffs (set at filter gain ≈-3 dB) around 250, 300, 350, 450 and 575 MHz (see Fig. 8). The emittance growths are shown in Fig. 9 revealing that, for the filters that were used, a cutoff above 450 MHz was needed to provide efficient damping of the instability.

V. INFLUENCE OF NUMERICAL NOISE

To check the consistency of the calculations, simulations of bunches 36 and 37 were performed, initialized with a dump of the electron distribution from a POSINST run after the passage of bunch 35. If all is consistent, the emittance growth of bunch 36 from such a simulation should match the emittance growth predicted for the same bunch 36 by the simulation of the (35,36) pair that is reported in the previous section. However, the emittance growth of bunches 36 and 37 from the (36,37) run did match closely the ones from bunches 35 and 36 from the (35,36) run. Examination of the average electron density confirmed however that it was overall higher in the simulation of bunches (36,37) than in the one of bunches (35,36) as expected. This suggests that the higher growth observed in vertical emittance of the second bunch is not due to the 8% increase in electron density between the two bunches.

To investigate this apparent paradox, single bunch simulations were conducted with a bunch with four-fold symmetry, and initial electron macro-electrons (assumed to fill a uniform density $n_e = 10^{12}$ m^{-3}) being initialized (a) on a uniform grid; (b) randomly refreshed at each station; (c) using at each station the same random distribution generated at the first station; (d) same as (c) and adding at each station random, one cell wide vertical displacements; (e) same as (d), and flipping randomly at each station the sign of the electrons horizontal and vertical positions. Finally, (b) and (d) were repeated with additional smoothing of the electron charge density, effectively filtering short range noise.

The emittance growth obtained for each of theses cases is given in Fig. 10. With uniform loading (a), no seed is available for the vertical instability to develop and the small emittance growth is solely due to non-linear forces (note that the amount of growth may not be physical since the number of stations $N_s = 10$ is not sufficient to resolve the betatron motion, in addition to other approximation like macro-particle statistics and field discretization). With random loading, the vertical instability develops immediately if the distribution is refreshed with a different random load at each time step (b), but develops only around turn 300 if the same random distribution is used for the entire simulation (c). Adding short range randomness to the initial distribution (d) still results in an onset around turn 300. Randomly flipping the sign of the electrons horizontal and vertical positions (e), which generates randomness at longer ranges, is more potent at provoking a much earlier onset. Smoothing short range noise in the deposited electron density does not significantly modify the emittance growth, confirming that long range rather than short range noise is most effective at triggering the instability.

By comparing the results obtained in this section with the ones obtained in the preceding one, we conclude that the lower emittance growth observed on bunch 35 was

mostly due to injecting the same electron distribution at each time step (from a POSINST dump), resulting in vanishing long range shot-to-shot numerical noise, contrary to what was experienced by bunch 36 which was subject to a different distribution of electrons at each time step, due to the random nature of the gas ionization and secondary emission events which occur between the two bunches.

We note that while numerical statistical noise is leading to variable onset of the instability in the simulations, it does not alter the leading order of the growth rate, which is observed to be the same after the onset of the instability for the simulations with no feedback that were presented in this section. If it is important nonetheless that both bunches be put on an equal footing with regard to numerical noise, results from Fig. 10 suggest that a technique based on random flipping of transverse positions of the injected electrons may be applicable. However, our more recent work (to be presented elsewhere) shows that it is possible to perform on present parallel computers simulations of a full batch of bunches, which thus do not suffer from the artifact linked to numerical noise described in this section, as the build-up of the electrons is computed self-consistently together with the bunches dynamics, and thus each bunch sees a statistically different electron distribution at each ecloud station.

VI. CONCLUSION

The WARP-POSINST framework has been augmented to allow for self-consistent multi-bunch simulations of the interaction of beams with electron clouds. New features include mesh refinement, parallelization, secondary emission of electrons, background gas ionization, and an idealized feedback model. Simulations of two consecutive bunches circulating in the SPS showed effective damping of electron-cloud induced transverse instability, provided that the bandwidth of the feedback has a cutoff at or above 450 MHz.

No multi-bunch effects were detected for the parameters that were considered here, and analysis of the sensitivity of the onset of the instability to numerical noise reveals that care must be exercised in the initialization of electrons and/or the analysis of emittance growth of a succession of bunches. In more recent work (to be presented elsewhere), simulations of a full batch of bunches have been performed which do not suffer from the artifact linked to numerical noise described in this paper, as the build-up of the electrons is computed self-consistently together with the bunches dynamics, and thus each bunch sees a statistically different electron distribution at each ecloud station.

Initial comparisons with experiment show good qualitative and some quantitative agreement on key aspects of the observed instability [3]. Work is underway for implementing a more realistic feedback model in WARP-POSINST using the same prediction algorithm that is to be used in the actual hardware, as well as perform thorough comparisons between experimental data and fully self-consistent modeling of entire bunch trains.

VII. ACKNOWLEDGMENTS

The authors thank M. Venturini, J. D. Fox, C. H. Rivetta, W. Höfle, R. Secondo and J. M. Byrd for insightful discussions and comments, as well as D. P. Grote for support with the code Warp.

VIII. APPENDIX A - BENCHMARKING OF WARP VS POSINST

Runs were performed with WARP and POSINST for the evolution of an electron cloud slice in the middle of a dipole. The average electron density history is given in Fig. 15 for a POSINST run and three WARP runs in: (a) 2-D, (b) 3-D with 4 cells longitudinally and a length of $0.2\sigma_z$, and (c) 3-D with 16 cells longitudinally and a length of $0.8\sigma_z$, where σ_z is the beam RMS length. For the 3-D runs, periodic boundary conditions were applied longitudinally for fields and particles. Snapshots of colored electron density plots and vertical phase space are given in Fig. 12, taken at $t = 130$ns. These results demonstrate a very good degree of agreement for electron cloud build simulations between POSINST, WARP in 2-D, and WARP in 3-D.

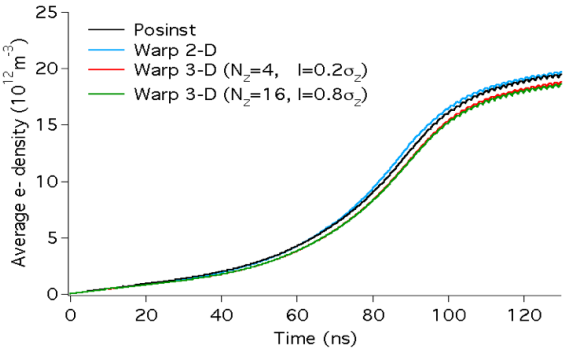

FIG. 11. Average electron density versus time from POSINST and WARP in build-up mode simulations.

IX. APPENDIX B - BENCHMARKING OF WARP VS HEADTAIL

An e-cloud driven instability was simulated in an LHC-like ring with WARP in a quasistatic mode, and the CERN code HEADTAIL using the parameters from table II in a drift (Fig. 13) and in a dipole (Fig. 14). Some of the parameters were purposely chosen to be unphysically large, so as to magnify their effects. The two codes

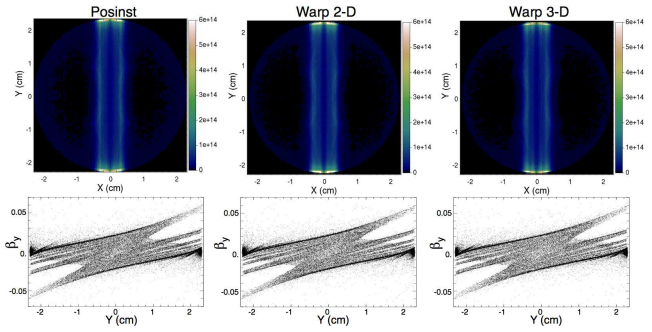

FIG. 12. Snapshots of electron density and vertical phase space from build-up simulations using (left) POSINST, (middle) WARP in 2-D, (right) WARP in 3-D.

TABLE II. Parameters used for simulations of e-cloud driven instability studies in the LHC.

circumference	C	26.659 km
beam energy	E_b	450 GeV
bunch population	N_b	1.1×10^{11}
rms bunch length	σ_z	0.13 m
rms beam sizes	$\sigma_{x,y}$	0.884, 0.884 mm
beta functions	$\beta_{x,y}$	66., 71.54 m
betatron tunes	$Q_{x,y}$	64.28, 59.31
chromaticities	$Q'_{x,y}$	1000., 1000.
synchrotron tune	ν	0.59
momentum compaction factor	α	0.347×10^{-3}
rms momentum spread	δ_{rms}	4.68×10^{-2}

predict similar emittance growth under the various conditions, with excellent qualitative agreement and good to very good quantitative agreement. Onset of instabilities are notoriously sensitive to small variations, and we tentatively attribute the quantitative discrepancies to differences in implementations including: adaptive (HEADTAIL) versus fixed (WARP) longitudinal grid sizes, different field solvers and particle pushers, different field interpolation procedures near internal conductors, slightly different values of physical constants, etc.

TABLE III. Parameters used for simulations of e-cloud effects study in the SPS.

circumference	C	6.911 km
beam energy	E_b	120 GeV
bunch population	N_b	1.1×10^{11}
rms bunch length	σ_z	0.184 m
rms beam sizes	$\sigma_{x,y}$	0.905, 1.32 mm
rms momentum spread	δ_{rms}	0.43×10^{-3}
beta functions	$\beta_{x,y}$	33.85, 71.87 m
betatron tunes	$Q_{x,y}$	26.13, 26.185
chromaticities	$Q'_{x,y}$	0.1, 0.1
synchrotron tune	ν	3.23×10^{-3}
momentum compaction factor	α	1.2566×10^{-3}

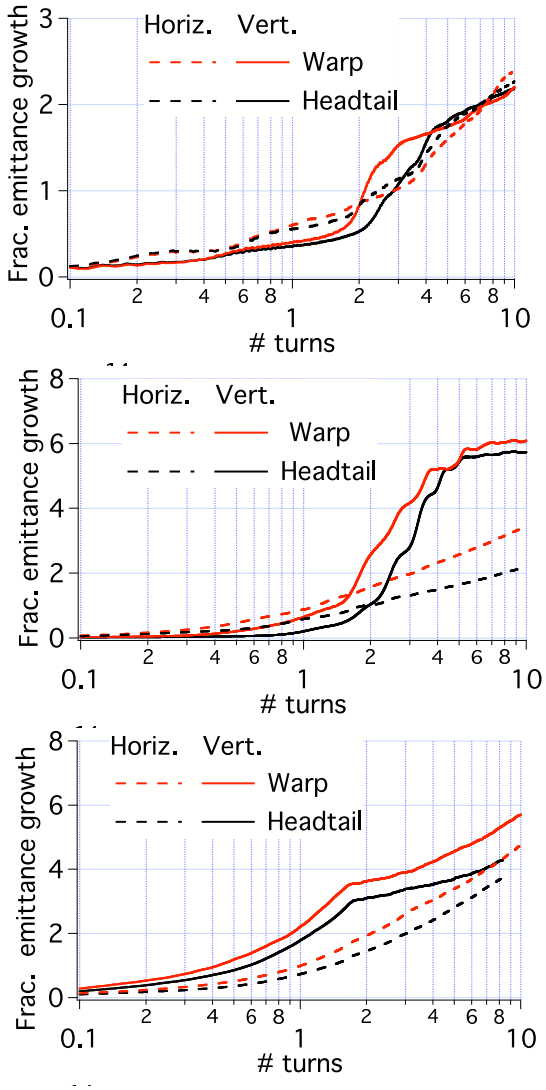

FIG. 13. Fractional emittance growth from WARP (red) and HEADTAIL (black) simulations of an e-cloud driven instability in drifts of an LHC-like ring for an electron background density of $10^{14} m^{-3}$ for (top) $\nu = \alpha = \delta_{rms} = Q'_x = Q'_y = 0$, (middle) $Q'_x = Q'_y = 0$, (bottom) parameters from table II.

Finally, WARP and HEADTAIL were used to simulate an electron cloud driven transverse instability in the SPS for a bunch at intermediate energy of 120 GeV, using the parameters given in table III. Both codes used a continuous focusing model for the transverse and longitudinal dynamics of the beam in the lattice. In addition, HEADTAIL had the option to apply a longitudinal focusing using a smooth function having the periodicity of the ring circumference, offering a more realistic localized focusing. The continuous versus localized longitudinal focusing in HEADTAIL are controlled by the input parameter "isyn", taking the values 1 and 4 respectively. For these runs, there was 10 electron cloud stations per turn, and the transverse simulation box size was $20\sigma_x \times 20\sigma_y$.

Fig. 15 shows the beam fractional emittance growth

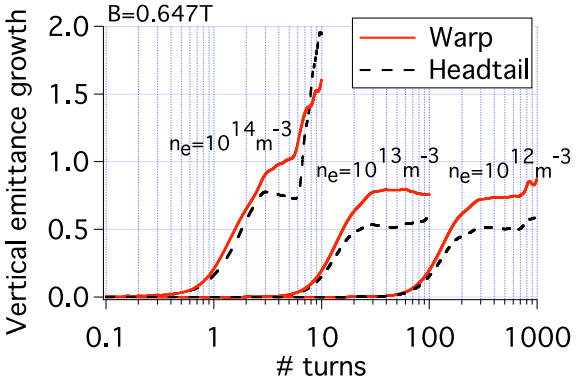

FIG. 14. Fractional vertical emittance growth from WARP and HEADTAIL simulations in dipoles of an LHC-like ring for three assumed initial electron densities.

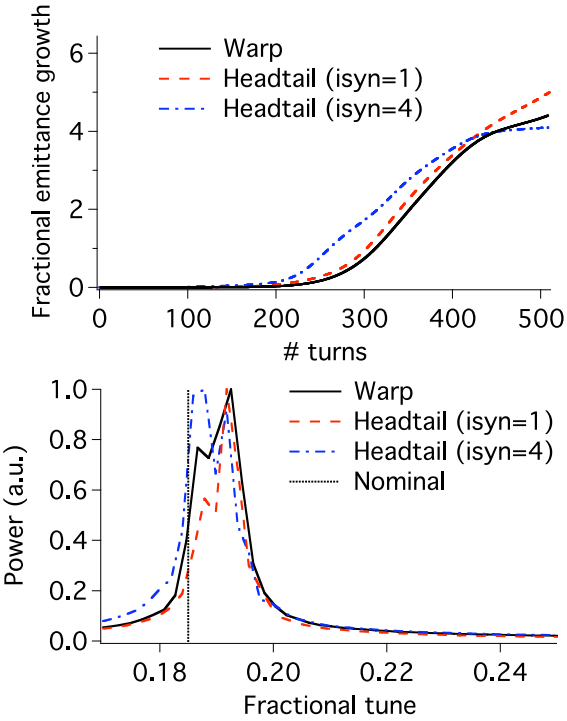

FIG. 15. Beam emittance versus turn number (top) and normalized power versus fractional tune (bottom) from computer simulations of electron cloud driven instability using the codes WARP and HEADTAIL. On the bottom plot, a dotted line indicates the location of the nominal vertical fractional betatron tune (0.185).

versus turn number and the normalized power versus fractional tune for simulations using a uniform electron density of $n_e = 1 \times 10^{12}$ m^{-3}. There is significant emittance growth, due to a transverse instability seeded by random particle noise. The three runs are in good agreement on the amount of emittance growth as well as on the average tune shift.

[1] Proc. International Workshop on Electron-Cloud Effects "ECLOUD07" (Daegu, S. Korea, April 9-12, 2007). http://chep.knu.ac.kr/ecloud07
[2] J. Fox et al., Proceedings Particle Accelerator Conference PAC09, Vancouver, Canada, paper TH6REP078 (2009)
[3] J. D. Fox et al., "SPS Ecloud Instabilities - Analysis of machine studies and implications for Ecloud Feedback", Proceedings First International Particle Accelerator Conference IPAC10, Kyoto, Japan, paper WEPEB052 (2010).
[4] G. Arduini et al., CERN-2005-001, 31-47 (2005)
[5] J-L Vay et al., "Simulation of a feedback system for the attenuation of e-cloud driven instability", Proceedings Particle Accelerator Conference PAC09, Vancouver, Canada, paper FR5RFP077 (2009).
[6] J. R. Thompson et al., "Initial results of simulation of damping system for electron cloud-driven instabilities in the CERN SPS", Proceedings Particle Accelerator Conference PAC09, Vancouver, Canada, paper FR5RFP076 (2009).
[7] JL Vay et al, Particle Accelerator Conference, Knoxville, TN, papers ROPB006 and FPAP016 (2005)
[8] M. A. Furman et al, Particle Accelerator Conference, Albuquerque, NM, paper TUXAB03 (2007)
[9] M. A. Furman and G. R. Lambertson, LBNL-41123/CBP Note-246, PEP-II AP Note AP 97.27 (Nov. 25, 1997). Proc. Intl. Workshop on Multibunch Instabilities in Future Electron and Positron Accelerators "MBI-97" (KEK, 15-18 July 1997; Y. H. Chin, ed.), KEK Proceedings 97-17, Dec. 1997, p. 170.
[10] M. A. Furman and M. T. F. Pivi, LBNL-49771/CBP Note-415 (Nov. 6, 2002). PRST-AB 5, 124404 (2003), http://prst-ab.aps.org/pdf/PRSTAB/v5/i12/e124404.
[11] M. A. Furman and M. T. F. Pivi, LBNL-52807/SLAC-PUB-9912 (June 2, 2003).
[12] M. A. Furman, LBNL-41482/CBP Note 247/LHC Project Report 180 (May 20, 1998).
[13] P. Sprangle, E. Esarey, and A. Ting, *Phys. Rev. Letters* **64**, 2011-2014 (1990).
[14] G. Rumolo and F. Zimmermann, *PRST-AB* **5** 121002 (2002).
[15] C. Huang, V.K. Decyk, C. Ren, M. Zhou, W. Lu, W.B. Mori, J.H. Cooley, T.M. Antonsen, Jr. and T. Katsouleas, *J. of Comput. Phys.* **217**, 658-679 (2006).
[16] B. Feng, C. Huang, V. Decyk, W.B. Mori, P. Muggli, T. Katsouleas, *J. of Comput. Phys.* **228**, 5340-8 (2009)
[17] K. Ohmi, Single Bunch Electron Cloud Instability for a Round Beam (Memo), 19. Nov. 2002.
[18] M. T. F. Pivi, "CMAD: a new self-consistent parallel code to simulate the electron cloud build-up and instabilities", Proceedings Particle Accelerator Conference PAC07, Albuquerque, NM, paper THPAS066 (2007)
[19] D. P. Grote, A. Friedman, J.-L. Vay. I. Haber, AIP Conf. Proc. 749 (2005) 55.
[20] J.-L. Vay, *Phys. Rev. Lett.*, **98** 130405 (2007)
[21] J.-L. Vay, *Phys. Plas.*, **15** 056701 (2008)
[22] J.-L. Vay et al, "Application of the reduction of scale range in a Lorentz boosted frame to the numerical simulation of particle acceleration devices", Proceedings Particle Accelerator Conference PAC09, Vancouver, Canada, paper TU1PBI04 (2009)
[23] J-L Vay et al., Update on e-cloud simulations using the package WARP/POSINST, PAC09, Proceedings, (2009).
[24] J. M. Byrd, Simulations of the PEP-II transverse coupled-bunch feedback system, PAC95, Proceedings, (1996).
[25] M. A. Furman and G. R. Lambertson, KEK Proceedings 97-17, p. 170. M. A. Furman and M. T. F. Pivi, PRSTAB/v5/i12/e124404 (2003).